Seismic assessment and retrofitting measures of a historic stone masonry bridge

Emmanouil N. Rovithis[*1] and Kyriazis D. Pitilakis[2]

[1]*Institute of Engineering Seismology and Earthquake Engineering (EPPO-ITSAK), Dasyliou Str., Elaiwnes, Pylaia, 55102, Thessaloniki, Greece*
[2]*Department of Civil Engineering, Aristotle University of Thessaloniki, 54124, Thessaloniki, Greece*

Abstract. The 750 m long "De Bosset" bridge in the Cephalonia Island of Western Greece, being the area with the highest seismicity in Europe, was constructed in 1830 by successive stone arches and stiff block-type piers. The bridge suffered extensive damages during past earthquakes, such as the strong M7.2 earthquake of 1953, followed by poorly-designed reconstruction schemes with reinforced concrete. In 2005, a multidisciplinary project for the seismic assessment and restoration of the "De Bosset" bridge was undertaken under the auspices of the Greek Ministry of Culture. The proposed retrofitting scheme combining soil improvement, structural strengthening and reconstruction of the deteriorated masonry sections was recently applied on site. Design of the rehabilitation measures and assessment of the pre- and post-interventions seismic response of the bridge were based on detailed in-situ and laboratory tests, providing foundation soil and structural material properties. In-situ inspection of the rehabilitated bridge following the strong M6.1 and M6.0 Cephalonia earthquakes of January 26th and February 3rd 2014, respectively, revealed no damages or visible defects. The efficiency of the bridge retrofitting is also proved by a preliminary performance analysis of the bridge under the recorded ground motion induced by the above earthquakes.

Keywords: retrofitting; "De Bosset" bridge; old stone masonry bridges; numerical analysis; micropiles; Cephalonia 2014 earthquakes

1. Introduction

The problem of retrofitting a two-hundred years old stone masonry bridge having sustained serious earthquake-induced damages followed by poorly-designed restorations requires consideration of a large number of parameters. The latter are related to the foundation soil conditions, the heterogeneity of construction materials, the existing strength and pathology of the structure and the identification of possible failure modes within assessment of the structure's vulnerability. The problem becomes more complex and challenging if the structure is exposed to high seismic risk, large traffic loads and unfavorable environmental conditions, while founded through rigid massive foundations on deformable soil, thus introducing soil-structure interaction as

*Corresponding author, Researcher Ph.D., E-mail: rovithis@itsak.gr

a key mechanism in controlling the dynamic characteristics of the structure and the effective seismic motion (Page 1993, Barros and Luco 1995, Proske and Van Gelder 2009, Asteris *et al*. 2014, Preciado *et al*. 2015). In this regard, a successful rehabilitation scheme should balance between structural integrity upgrade aligned to design codes requirements and maintenance of the bridge monumental features. For this reason, a comprehensive set of available in-situ inspections, field measurements and earthquake recordings are of major importance to assess the pathology and select the most appropriate retrofitting scheme for such type of monumental structures (Krstevska *et al*. 2008, Cakir and Seker 2015).

A well-documented case study dealing with the design of an innovative retrofitting scheme to meet both structural safety requirements and architectural needs of the historic stone masonry "De Bosset" bridge in the Cephalonia Island of Western Greece is presented in this paper. The pre-rehabilitation seismic stability of the bridge in terms of transverse structural strength and bearing capacity of the foundation soil is estimated by a fracture line approach and a stress-based seismic analysis of a three-dimensional finite-element model, respectively. Foundation soil properties are defined by field surveys and laboratory tests. The design seismic motion at the foundation level of the bridge is determined from soil response analysis accounting for non-linear soil behavior under selected ground motions recorded in close distance from the bridge site at the time of the study. Soil compliance is modeled by means of Winkler spring supports to evaluate soil-structure interaction effects by comparing the seismic response between fixed- and flexible-base (compliant) bridge models in the realm of elastodynamic considerations. Based on the identified pathology and the critical zones of the bridge, a set of intervention measures is proposed by combining foundation soil improvement, strengthening of the bridge stability under transverse loading and maintenance of its monumental nature. The proposed rehabilitation works were recently completed, providing an overall seismic upgrade of the bridge. The latter is proved by the very good seismic performance of the rehabilitated bridge following the two strong M6.1 and M6.0 earthquakes of January 26th and February 3rd, 2014, respectively, that stroke Cephalonia inducing particularly high ground accelerations. Besides post-earthquake field inspection, further support on the effectiveness of the intervention scheme is provided from numerical analyses of the rehabilitated bridge by implementing the actual seismic loading induced by the two earthquakes.

The study presented herein was performed in the framework of a multidisciplinary project under the auspices of the Directorate for the Restoration of Byzantine and Post-byzantine Monuments of the Greek Ministry of Culture (Pitilakis 2006, Rovithis and Pitilakis 2011).

2. Historical background

Originally constructed in 1830 by successive stone arches founded on stiff block-type stone piers, the historic multi-span stone masonry "De Bosset" bridge connects the shorelines of Argostoli and Drapano at the southern side of the Argostoli bay (Fig. 1). The bridge has a total length of 750 m and its height varies between 2 to 4 m along its longitudinal axis. The foundation area of the bridge piers is approximately equal to 10 m long and 5 m wide. The severe $M_s7.2$ earthquake of 1953 (Papazachos 1997) induced extensive deformations of the deck and differential settlement of the piers (Fig. 2(a)). The characteristic failure mechanism of old stone bridges related to out-of-plane collapse of the arch walls and filling material (Griffith *et al*. 2003) is evident in Fig. 2(b). Major parts of the bridge were totally reconstructed during the period of 1960 to 1970. The original stone sections and the filling material of the bridge were removed (Fig. 2(c)). A new

Fig. 1 Overview of the old stone masonry 750 m long "De Bosset" bridge in Cephalonia island connecting the city of Argostoli with the opposite shoreline (Drapanos) (Google earth image)

reinforcement mesh was installed to form the arch-shaped sections of the bridge (Fig. 2(d)) and two new concrete spandrel walls of approximately 40 cm width were cast in place (Fig. 2(e)). In this manner, the original architectural pattern of the bridge was reproduced by reinforced concrete (Fig. 2(f)) while modifying substantially the material homogeneity and structural stiffness of the bridge. However, the extent of the above interventions along the longitudinal axis of the bridge is unknown since the authentic dry stone material was preserved in some sections of bridge including the first two arches close to the city of Argostoli. The latter is illustrated in the photogrammetric mapping of a part of the western façade of the bridge shown in Fig. 3.

3. Pathology of the bridge

In 2005, a multidisciplinary research project for the seismic assessment and restoration of the "De Bosset" bridge was undertaken by the Laboratory of Soil Mechanics, Foundation and Geotechnical Earthquake Engineering (LSMFGEE) of the Aristotle University of Thessaloniki (Pitilakis 2006) and supervised by the Directorate for the Restoration of Byzantine and Post-byzantine Monuments of the Greek Ministry of Culture. A series of in-situ inspections and laboratory tests on concrete and stone specimens was performed to obtain a detailed knowledge of the bridge pathology and strength. With reference to structural defects, extensive cracks up to 20 cm wide and 40 cm deep were recorded in the tensile zones under the arches (Fig. 4(a)). An underwater inspection revealed large foundation scouring up to 1m deep in most of the bridge

piers (Fig. 4(b)), due to strong sea currents within the Argostoli bay. The original stone masonry material was highly deteriorated by deep corrosion, loss of mass and poor condition of joint mortars. Delamination and detachment of covering was observed for the concrete sections. Laboratory tests on concrete specimens revealed a substantially low compressive strength corresponding to concrete category C8/10, whereas the effective cross section of the reinforcement bars was reduced to almost one half of the original section area. Mean values for the static modulus of elasticity were measured at 10 GPa. Further details on the above experimental data may be found in Papayianni *et al*. (2007).
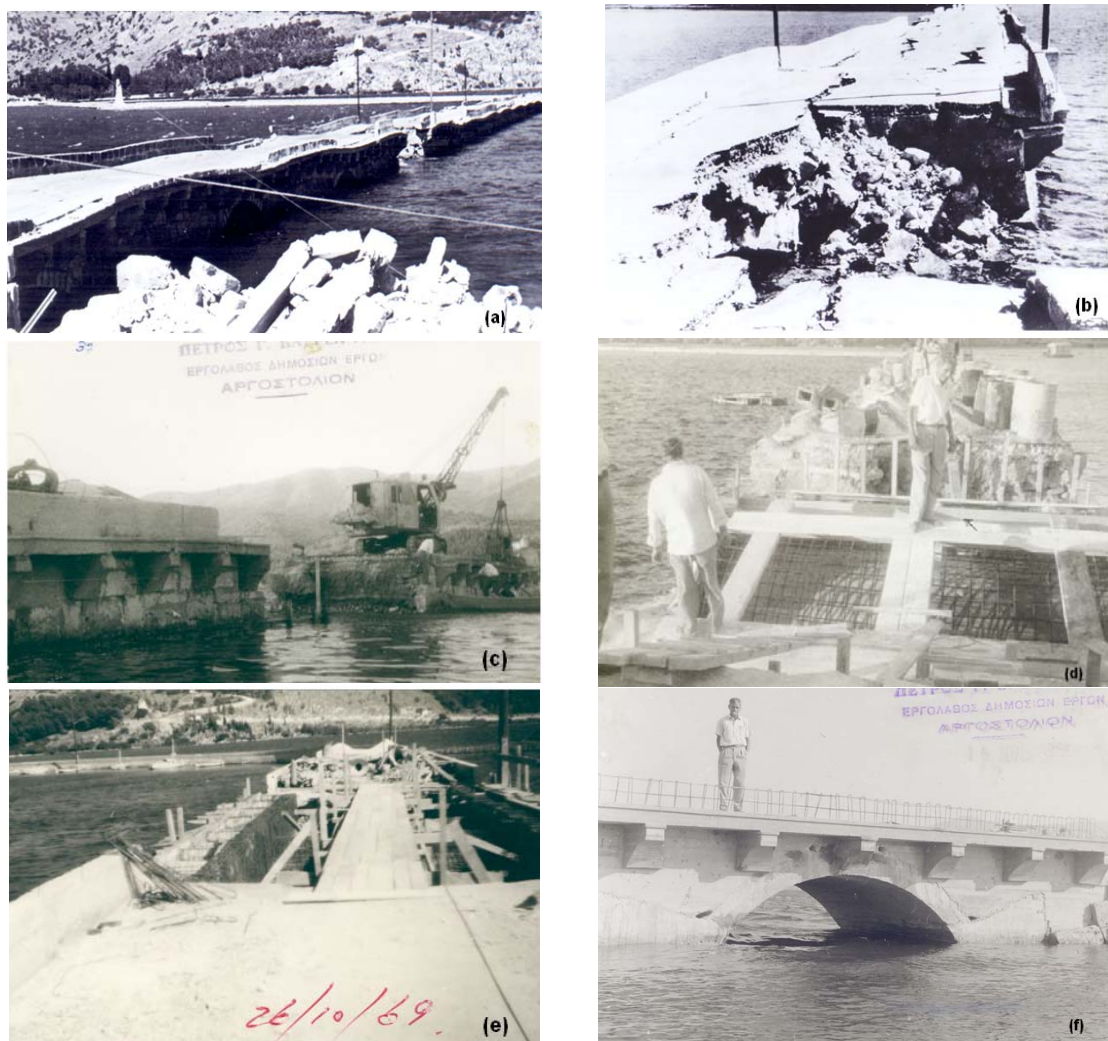
Fig. 2 (a), (b) Extensive damages to the "De Bosset" bridge due to the severe M_s7.2 earthquake of 1953, including lateral deformations and differential settlement of the deck and out-of-plane collapse of the arch walls and filling material; (c)-(f) partial reconstruction of the bridge with reinforced concrete during the period 1960-1970; (c) removal of the original stone sections and the filling material; (d), (e) placement of the reinforcement forming the original shape of the bridge arches (f) a typical arch of the bridge reconstructed with reinforced concrete
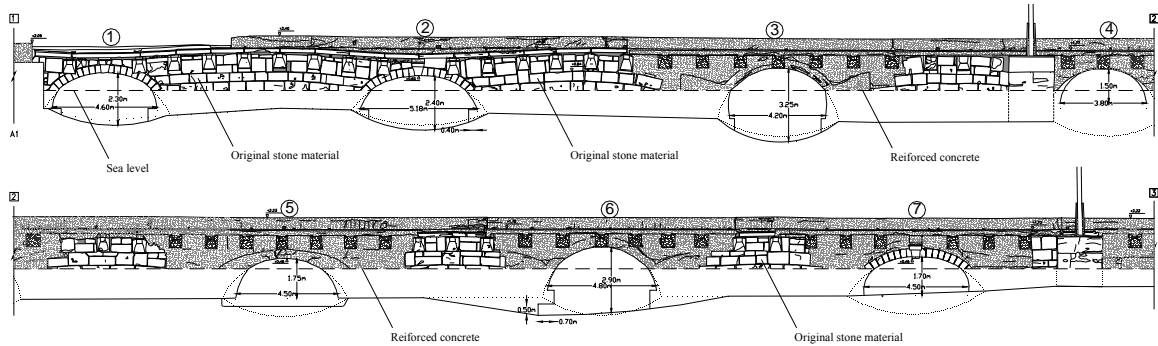
Fig. 3 Western façade of the bridge along the first seven arches close to Argostoli city based on photogrammetric mapping (The photogrammetric study was conducted in 2002 by the Photogrammetry Lab of the School of Rural and Surveying Engineering of the National Technical University of Athens)
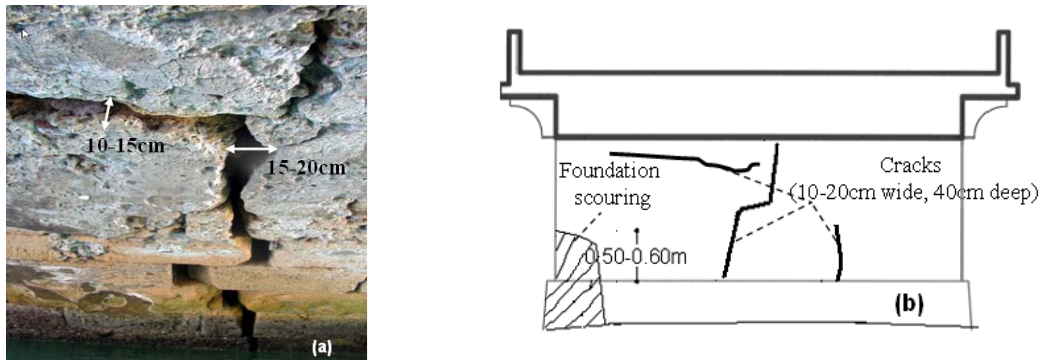
Fig. 4 Typical findings during the in-situ inspection of the bridge pathology in 2005: (a) Extensive longitudinal and transverse cracks in the tensile zones under the arches and (b) foundation scouring of the piers base
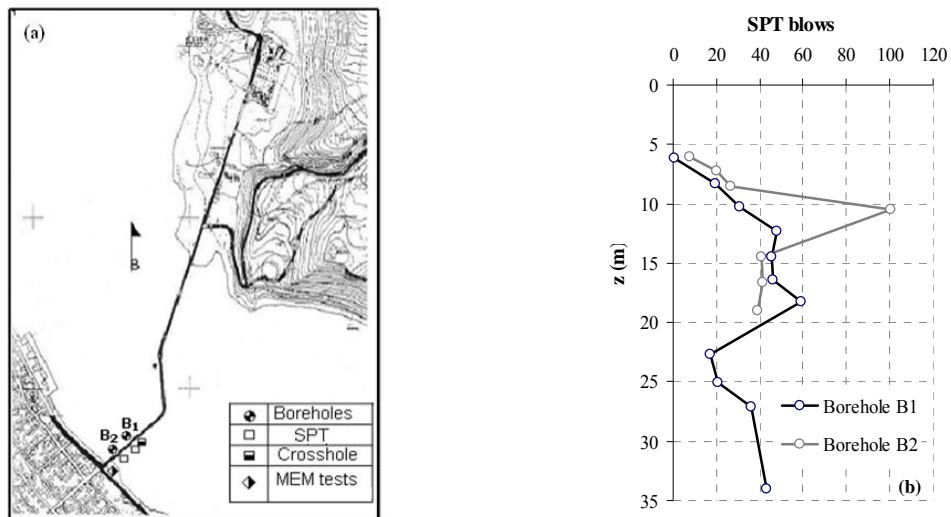
Fig. 5 (a) Geotechnical and geophysical tests performed along the "De Bosset" bridge in 2005, (b) SPT test results obtained at B1 and B2 boreholes location

4. Geotechnical and geophysical investigation

The geotechnical and geophysical field campaign comprised of geotechnical borings, Standard Penetration Testing (SPT), Cross-Hole Seismic (CH) and Microtremor Array Measurements (MAM) at selected locations along the bridge shown in Fig. 5(a). SPT profiles at boreholes B1 and B2 are plotted in Fig. 5(b). The field surveys were complemented with laboratory tests to provide the mechanical and the dynamic properties of the foundation soil. The geotechnical cross section of the bridge site obtained from the in-situ surveys is illustrated in Fig. 6. The local sandstone, which can be considered as the seismic bedrock with shear wave propagation velocity (V_s) larger than 1000 m/s, is found at a depth of about 35 m. It is overlaid by a soft silty clay layer of low shear strength with V_s varying between 140 and 170 m/s. The measured angle of friction (φ_u) and cohesion (c_u) of the surficial layer under undrained loading conditions are 3° and 26.1 KPa, respectively, while the average plasticity index (PI) is 30%. Considering the above characteristics, the foundation soil of the bridge should be classified as soil type D (i.e., soft clays of high plasticity index and thickness higher than 10 m) according to the Greek Seismic Code (EAK2000). Resonant column tests provided shear modulus (G) degradation and hysteretic damping ratio (D) curves of the soil layers with increasing shear strain (γ). The latter were adopted in equivalent linear soil response analyses, presented in the ensuing.

5. Design input motion and fundamental frequency of soil

In order to estimate the design seismic motion at the foundation level of the bridge, a well-documented set of twenty five earthquakes with magnitude (M_s) and peak horizontal ground acceleration (PHGA) ranging between 3.7 to 5.2 and 0.02 g to 0.2 g, respectively, were selected to estimate the rock outcrop motion. The above earthquakes were recorded in the period of 1999 to 2003 by an accelerometric station, hereafter referred as CH station, installed at the Cephalonia Greek Telecommunication building (OTE), 500m away from the bridge site. The CH station was operated and maintained by ITSAK (www.itsak.gr) as part of the Greek National Accelerometric Network until 2012, when the CH station was replaced by a new 24 bit accelerometric station (ARG2) installed at the basement of a two-story building, owned by the Prefecture authority of the Ionian Islands (EPPO-ITSAK report 2014a). Further details on the ARG2 station are reported in the ensuing subsoil conditions at the CH station site are available from earlier studies (AUTH-ITSAK report 1996) based on SPT and CH tests.

Upon implementing the shear wave velocity profile at CH station site, a series of deconvolution analyses were performed to derive the rock outcrop motion for each one of the selected earthquake records. The computed rock motions were scaled to 0.36 g, corresponding to the design acceleration for the seismic zone III which includes the island of Cephalonia according to the Greek Seismic Code EAK2000. The scaled rock motions were then specified at the seismic bedrock (i.e., V_s>1000 m/s) defined at -35 m of the bridge soil profile. One-dimensional equivalent linear ground response analyses were then performed by implementing the finite-element code Cyberquake (Modaressi and Foerster 2000) to compute soil response at the ground surface of the bridge site. For this reason, the experimental G-γ-D curves mentioned above were employed. Based on the geotechnical cross section derived from the in-situ geophysical tests (Fig. 6), three shear wave velocity profiles grouped as "A1-A4", "A5-A9" and "A10-A15" (Fig. 7(a)) were adopted to model the variation of the foundation soil stiffness along the bridge longitudinal axis.
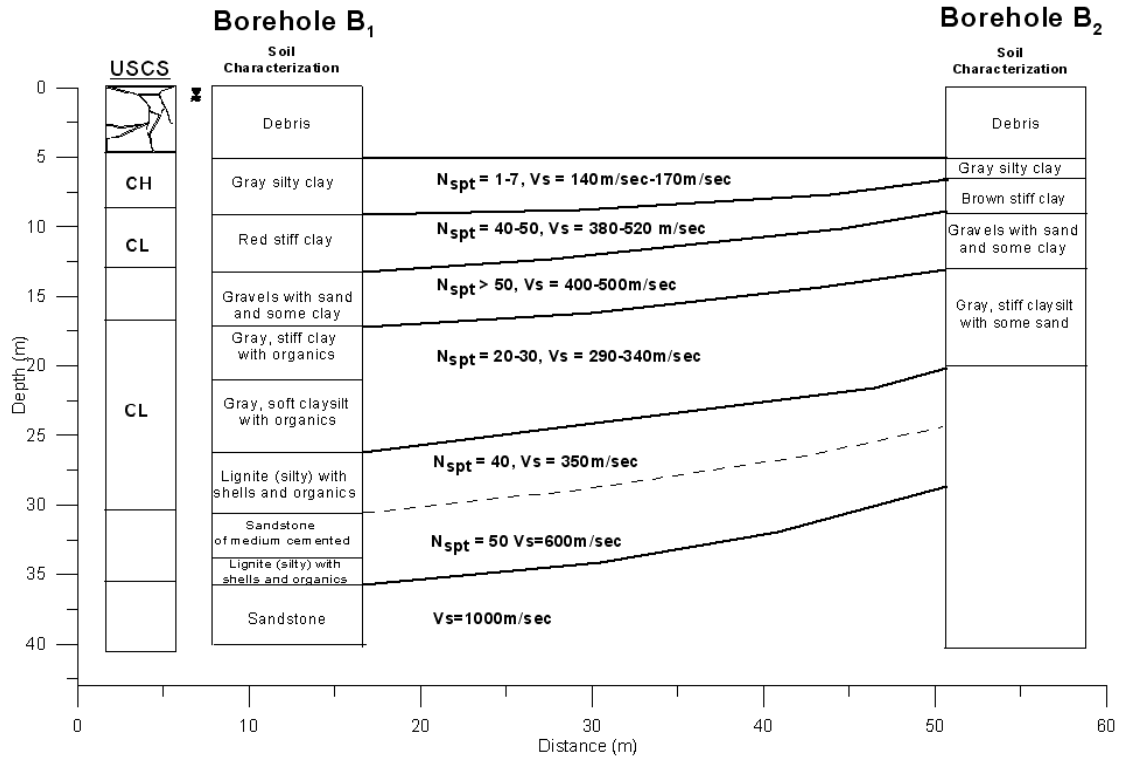
Fig. 6 Geotechnical cross section of the bridge foundation soil along the line B1-B2 shown in Fig. 5(a)
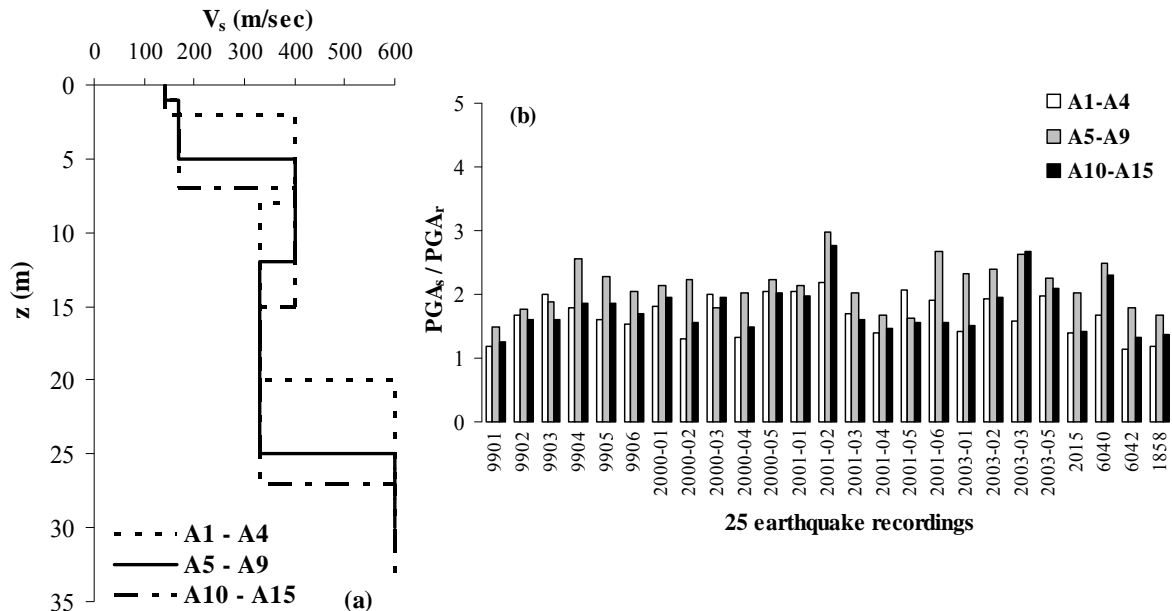
Fig. 7 (a) Shear wave propagation velocity (V_s) profiles to account for variation of V_s along the bridge longitudinal axis. (b) Surface-to-bedrock peak acceleration ratios (PGA_s/PGA_r) at the bridge site for each one of the 25 selected earthquake recordings
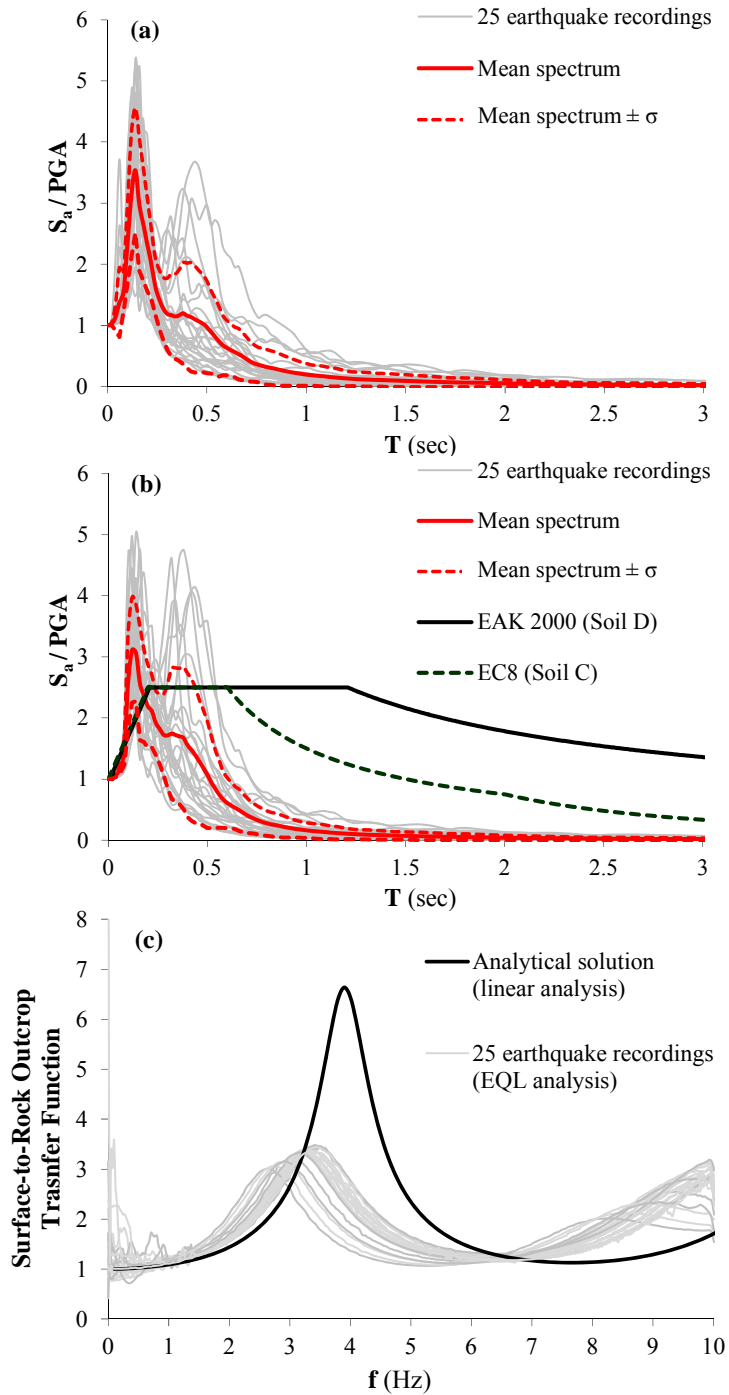
Fig. 8 Normalized acceleration response spectra at (a) bedrock level and (b) ground surface of the bridge soil profile computed from equivalent linear soil response analysis. EAK2000 and EC8 normalized elastic spectrum corresponding to soil category D and C, respectively, are also plotted. (c) Comparison of surface-to-rock outcrop transfer functions between damped (d=10%) linear elastic solution (Roesset 1977) and equivalent linear analyses. The graphs refer to the "A1-A4" V_s model

The corresponding surface-to-bedrock peak acceleration ratios (PGA_s/PGA_r) are plotted in Fig. 7(b). Each code name in the abscissa of the graph refers to a selected earthquake event. A mean PGA_s/PGA_r ratio at 1.7 was revealed, corresponding to a mean peak horizontal acceleration of 0.6 g at the ground surface of the bridge soil profile. It is noted that, stronger amplification of the seismic motion from bedrock to ground surface was observed for the deeper soil models "A5-A9" and "A10-A15". Figs. 8(a) and 8(b) shows the normalized acceleration response spectra computed at the bedrock and the ground surface, respectively, referring to the "A1-A4" shear wave velocity model. The high frequency content of the computed earthquake motions is reflected in the mean response spectrum compared with the elastic design spectrum of EAK2000 and EC8 (CEN 2002) for soil category D and C, respectively. Surface-to-rock outcrop transfer functions obtained from the equivalent linear analyses are compared in Fig. 8(c). The analytical solution reported in Roesset (1976) for a multi-layer damped (d=10%) soil is also plotted, denoting a fundamental frequency (f_o) of the bridge soil deposit at 4 Hz under linear viscoelastic considerations. Evidently, the degradation of soil stiffness and damping increase with increasing shear strains γ shifted f_o to lower frequencies in the range of 2.5 to 3.5 Hz, depending on the frequency characteristics of the input motion.

6. Transverse structural stability

Mention has already been made to the extensive longitudinal and transversal cracks that were observed under the stone arches, indicating poor structural stability. The fracture line method reported in Erdogmus and Boothby, 2004 was employed to evaluate the transverse strength of the bridge under seismic loading. The above method is originated from the yield line theory that has been adopted in code provisions (British Standards 1992) for unreinforced masonry design. In this case, the spandrel wall is considered as a retaining wall of the material fill volume above the arch, inducing active-state pressures as applied loads. In fracture line analysis, the yield lines on a surface, representing axes of rotation, are the equivalent of hinges on a beam that occur when the plastic bending moment is reached (Erdogmus and Boothby 2004). The bending moment producing rupture is assigned to all points along a hinge line. The selected fracture line pattern representing the failure mechanism, depends on the boundary conditions, geometry and material properties of the problem at hand. In the case of the "De Bosset" bridge, the assumed fracture line pattern is shown in Fig. 9, resembling the out-of-plane collapse of the spandrel walls caused by the 1953 earthquake (Figs. 2(a) and 2(b)). According to the above method, the maximum allowable pressure q_{max}, referring to the transverse strength of the wall, may be estimated from the equivalence of external and internal work

$$\sum W_i = \sum W_e \tag{1}$$

where W_i is the internal work done by the resisting wall, given by

$$\sum W_i = \sum M_f l\theta \tag{2}$$

and W_e stands for the external work done by the applied loads as follows

$$\sum W_e = \sum Q\theta d \tag{3}$$
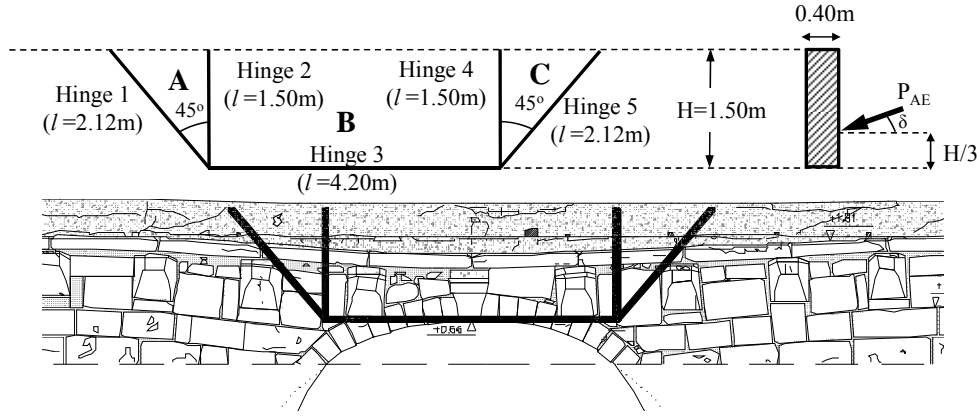
Fig. 9 Assumed fracture line pattern of a typical bridge arch for estimating transverse load effects by means of the fracture line method reported in Erdogmus and Boothby (2004). The adopted fracture line pattern resembles that of the out-of-plane collapse pattern of the "De Bosset" induced by the 1953 earthquake

Table 1 Simplified assessment of the bridge transverse stability based on the fracture line method reported in Erdogmus and Boothby (2004)

Internal Work calculations					
Panel	Hinge	l (m)	θ	$M_f=f_rS$ (KNm/m)	$W_i=M_fl\theta$ (KNm)
A	1	2.12	$\theta\sqrt{2}$	4.32	13.81θ
	2	1.5	θ	4.32	$6.91\,\theta$
B	3	4.2	θ	4.32	$18.14\,\theta$
C	4	1.5	θ	4.32	$6.91\,\theta$
	5	2.12	$\theta\sqrt{2}$	4.32	$13.81\,\theta$
				$\Sigma W_i=$	57.01θ

External Work calculations					
Panel	l (m)	H (m)	θ	Q (KN)	d (m)	$W_e=Qd\theta$ (KNm)
A	1.5	1.5	$\theta\sqrt{2}$	$q_{max}l\,H/6 =$ 0.375q_{max}	$H/2 =$ 0.75	0.397 $q_{max}\,\theta$
B	4.2	1.5	θ	$q_{max}l\,H/2 =$ 3.15q_{max}	$H/3 =$ 0.5	1.58 $q_{max}\,\theta$
C	1.5	1.5	$\theta\sqrt{2}$	$q_{max}l\,H/6 =$ 0.375q_{max}	$H/2 =$ 0.75	0.397 $q_{max}\,\theta$
					$\Sigma W_e=$	2.37 $q_{max}\,\theta$
Maximum allowable pressure q_{max} (KPa)=$\Sigma W_i/\Sigma W_e$						**24.05**

Active-state earth pressures (Mononobe-Okabe method)						
H (m)	k_h/g k_v/g	$\varphi(°)/\delta(°)$	$\psi(°)$	K_{AE}	P_{AE}(KN/m)	q_{AE} (KPa)
1.5	0.6 0.25	37/18.5	38.7	1.738	25.2	**33.6**
Safety factor against shear failure $SF_s=q_{max}/q_{AE}$						**0.71**

In the above equations, $M_f(=f_rS)$ is the bending moment producing fracture, f_r is the tensile strength of the stone masonry, S stands for the section modulus of the wall, l is the length of the fracture line, θ is the rotation along the fracture line, Q refers to the resultant force imposed by the external loads and d is the distance from the point of application of Q to the facture line.

Upon substituting W_e and W_i in Eq. (1), it may be rewritten as

$$\sum (f_rS)l\theta = \sum Q\theta d \qquad (4)$$

With reference to the external seismic loading imposed on the bridge spandrel wall, the resultant lateral active thrust P_{AE} (Fig. 9) is estimated by implementing the Mononobe-Okabe approach (Okabe 1924, Mononobe and Matsuo 1929). For this reason, the coefficient of horizontal acceleration (k_h/g) of the backfill was set at 0.6, taking into account the abovementioned mean peak horizontal acceleration computed at the ground surface of the bridge soil profile, whereas the coefficient of vertical acceleration (k_v/g) was set at $0.42k_h$.

The above calculations are summarized in Table 1, where the Q and d values refer to a triangular soil pressure distribution. The ratio (q_{max}/q_{AE}) of the maximum allowable pressure (q_{max}) over the active seismic earth pressure (q_{AE}) yields a safety factor against transverse structural stability equal to 0.7, indicating a critical transverse condition of the bridge that should be encountered in the design of the rehabilitation measures.

7. Safety factor against bearing capacity of the foundation soil

Within a second, more rigorous analysis stage of the bridge seismic response, a three-dimensional finite element model was analyzed in the frequency domain by implementing the finite-element code ANSYS (ANSYS 2001). In order to reduce computational cost, a representative part of the bridge (Fig. 10) was modelled with proper boundary conditions to obtain equivalent modal characteristics with the whole bridge (Rovithis *et al.* 2006, Rovithis and Pitilakis 2011). Cubic elements were employed to reproduce the actual geometry of the bridge by assuming perfect bonding between the elements in the framework of a stress-based analysis. The mean value of the elastic modulus of elasticity (E_s) obtained from laboratory tests at 10 GPa was adopted as a modelling approximation of the cracked and heterogeneous material of the bridge (OPCM 3274, 2005). Both fixed- and flexible-base models were analyzed to investigate soil-structure interaction
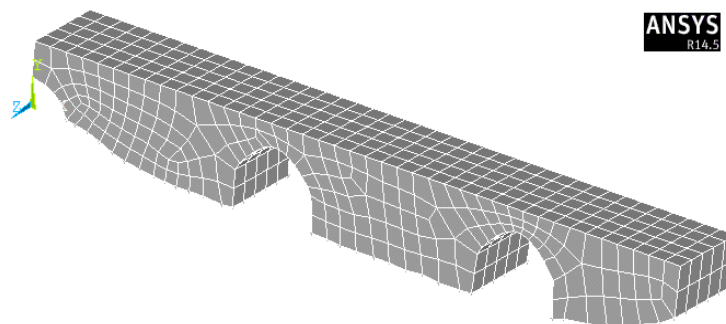
Fig. 10 Three-dimensional finite-element model of a representative part of the "De Bosset" bridge adopted for the stress-based analysis of the bridge seismic response

Table 2 Modal characteristics of the "De Bosset" bridge corresponding to (a) the fixed-base model (b) the flexible-base model before the rehabilitation measures and (c) flexible-base model after the rehabilitation measures. Results refer to mean elastic material properties (E_s=10 GPa) derived from laboratory tests (Papayianni *et al*. 2007)

Mode	(a) Fixed-base model		(b) Flexible-base model		(c) Flexible-base rehabilitated model	
	Frequency (Hz)	Mass fraction	Frequency (Hz)	Mass fraction	Frequency (Hz)	Mass fraction
1	35.67	0.645	1.68	0.705	2.15	0.881
2	39.38	0.646	3.78	0.745	4.51	0.882
3	47.62	0.813	3.91	0.997	6.23	0.996

Table 3 Modal characteristics of the "De Bosset" bridge corresponding to (a) the fixed-base model (b) the flexible-base model before the rehabilitation measures and (c) flexible-base model after the rehabilitation measures. Results refer to a reduced modulus of elasticity E'_s=0.1E_s

Mode	(a) Fixed-base model		(b) Flexible-base model		(c) Flexible-base rehabilitated model	
	Frequency (Hz)	Mass fraction	Frequency (Hz)	Mass fraction	Frequency (Hz)	Mass fraction
1	11.27	0.634	1.62	0.743	2.058	0.867
2	12.45	0.635	2.46	0.75	2.896	0.868
3	15.06	0.799	3.67	0.93	5.249	0.991

effects by means of Winkler spring supports introduced at the base of the bridge piers. For this reason, pertinent analytical formulas reported in Gazetas (1991) for computing the stiffness of surface foundations were adopted. It is reiterated that the foundation area of the bridge piers has plan dimensions 10 m×5 m.

7.1 Modal analysis

Modal characteristics of fixed- and flexible-base bridge models are summarized in Table 2, referring to the first three vibrational modes with a dominant translational component in the transverse direction. Note the particularly stiff first-mode response with a natural period at 0.03 sec under fixed-base conditions. The comparison of natural modes between fixed- and flexible-base models reveals a strong effect of soil-structure interaction by increasing the fundamental natural period of the bridge up to 0.6 sec for the flexible-base case. Similar observations on the vibrational characteristics of old stone bridges have been reported in Rota *et al*. (2005) and Brencich and Colla (2002) based on field measurements. The modal response of the rehabilitated bridge discussed in the ensuing, is also reported in Table 2. Given the highly deteriorated and heterogeneous load-resisting system of the "De Bosset" bridge, the modal response of the structure was re-examined under the assumption of a substantially lower modulus of elasticity E'_s of the bridge equal to 0.1E_s. Modal analysis results obtained for E'_s are summarized in Table 3, denoting

lower values of eigenfrequencies. However, strong effects of soil-structure interaction are observed in both cases, whereas comparable the first-mode natural frequencies are obtained under flexible-base conditions. For this reason, the seismic response of the bridge reported in the following sections corresponds to the modal response reported in Table 2, where E_s is set at 10 GPa.

7.2 Response spectrum analysis

Having identified the vibrational characteristics of the bridge, a series of response spectrum analyses were performed to estimate the vertical stress field under the bridge piers. The mean acceleration response spectra specified at the base of the bridge models were those computed from the free-field ground response analyses. Code-defined elastic spectra were also implemented as a conservative loading in the transverse direction (Rota *et al*. 2005). The mean vertical stress developed under the foundation area of a typical pier was compared with the bearing capacity of the foundation soil which in turn was computed from the available geotechnical data. The corresponding safety factor (SF_{soil}), referring to the ratio of the bearing capacity of the bridge foundation soil over the mean vertical stress developed under the bridge piers, is plotted in Fig. 11, for fixed- and flexible-base conditions, respectively. Each bar in the graph refers to a different loading spectrum obtained from soil response analysis ("A1-A4", "A5-A9" and "A10-A14" soil profiles) and code regulations (EAK2000 elastic spectrum for soil category D and EC8 elastic spectrum for soil category C). The deviation between fixed- and flexible-base model reflects the effect of soil-structure interaction on the vibrational characteristics of the structure and consequently on the imposed seismic loading. With reference to the pre-rehabilitated bridge, the safety factor related to the bearing capacity of the bridge foundation soil is below unity for both fixed- and flexible-base cases.

8. Rehabilitation measures

The computed safety factors against transverse structural strength and bearing capacity of the foundation soil indicated clearly that the retrofitting scheme should be oriented towards structural strengthening and foundation soil improvement of the bridge. Upon summarizing observations from the field inspections, the comprehensive field and laboratory tests and the seismic response analysis of the pre-rehabilitated bridge, it was decided that the retrofitting scheme should take into account:
   • The restoration of the original masonry authentic nature that was substantially corrupted by the interventions with reinforced concrete after the strong M7.2 earthquake of 1953.
   • The extensive longitudinal and transversal cracks in the tensile zones under the arches.
   • The deep corrosion, loss of mass and poor condition of joint mortars in the authentic stone material.
   • The delamination of the concrete sections and detachment of the covering.
   • The scoured foundation of the bridge piers.
   • The inadequate transverse strength of the bridge in case of a strong earthquake.
   • The low-strength and the insufficient bearing capacity of the compressible foundation soil.
   In this regard, the adopted rehabilitation scheme shown in Fig. 12 was based on the following design concepts: (a) maintenance of the monumental features of the bridge by partial or total

restoration of the detached stones and the concrete facades with local stones being compatible with the authentic material, (b) increase of the bridge transverse strength with highly-resistant mortar to connect the new stone elements and closely spaced stainless steel lateral tendons to confine the bridge spandrel walls along the longitudinal direction, (c) improvement of the foundation soil by a group of micropiles, designed as a complementary load-transfer mechanism, while increasing the bearing capacity of the foundation soil and (d) protection of the piers base against future scouring with stone-gravel material.

With reference to the foundation soil improvement, the final design of the rehabilitation measures (Pitilakis 2006) yielded for each bridge pier a group of twenty-two micropiles, drilled from the bridge deck until the stiff gravel-sand layer found at -10 m (Fig. 6). The pile diameter (D), the normalized pile spacing (S/D) and the pile length to pile diameter ratio (L/D) were set at 0.25 m, 8 and 60, respectively. The axial load capacity of each pile is 340 KN and 270 KN, referring to pile shaft friction and pile tip resistance, respectively, whereas the design axial load for each pile was computed at 300 KN for combined gravity and seismic loads. Given that shaft friction is considered as the main resisting mechanism of the micropiles, within the context of the proposed soil strengthening intervention, the above pile group configuration provides safe transmission of the bridge loads, by increasing the overall bearing capacity of the soil-micropiles group system. Piles longitudinal reinforcement detailing is composed of 12 steel bars of 16 mm diameter whereas piles transverse reinforcement is formed by 8 mm diameter spiral stirrups placed every 10 cm along the pile shaft. More densely-spaced stirrups were designed for the piles transverse reinforcement at the level of the bridge base and the interface between soil layers with different stiffness. Regarding strengthening of the bridge monolithic behaviour in the transverse direction, the design of the rehabilitation measures resulted in a series of 20 mm diameter stainless
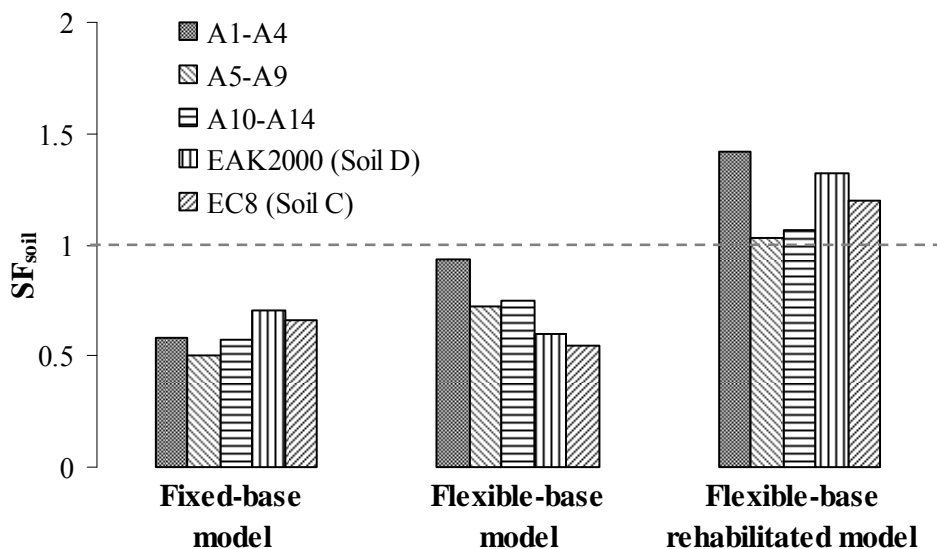
Fig. 11 Safety factor against bearing capacity of the bridge foundation soil; fixed-base model, flexible-base bridge model before the rehabilitation measures and flexible-base model after the rehabilitation measures. Each bar refers to a different spectrum loading derived from soil response analysis (A1-A4, A5-A9 and A10-A14 soil profiles) and code regulations (EAK2000 elastic spectrum for soil category D and EC8 elastic spectrum for soil category C)
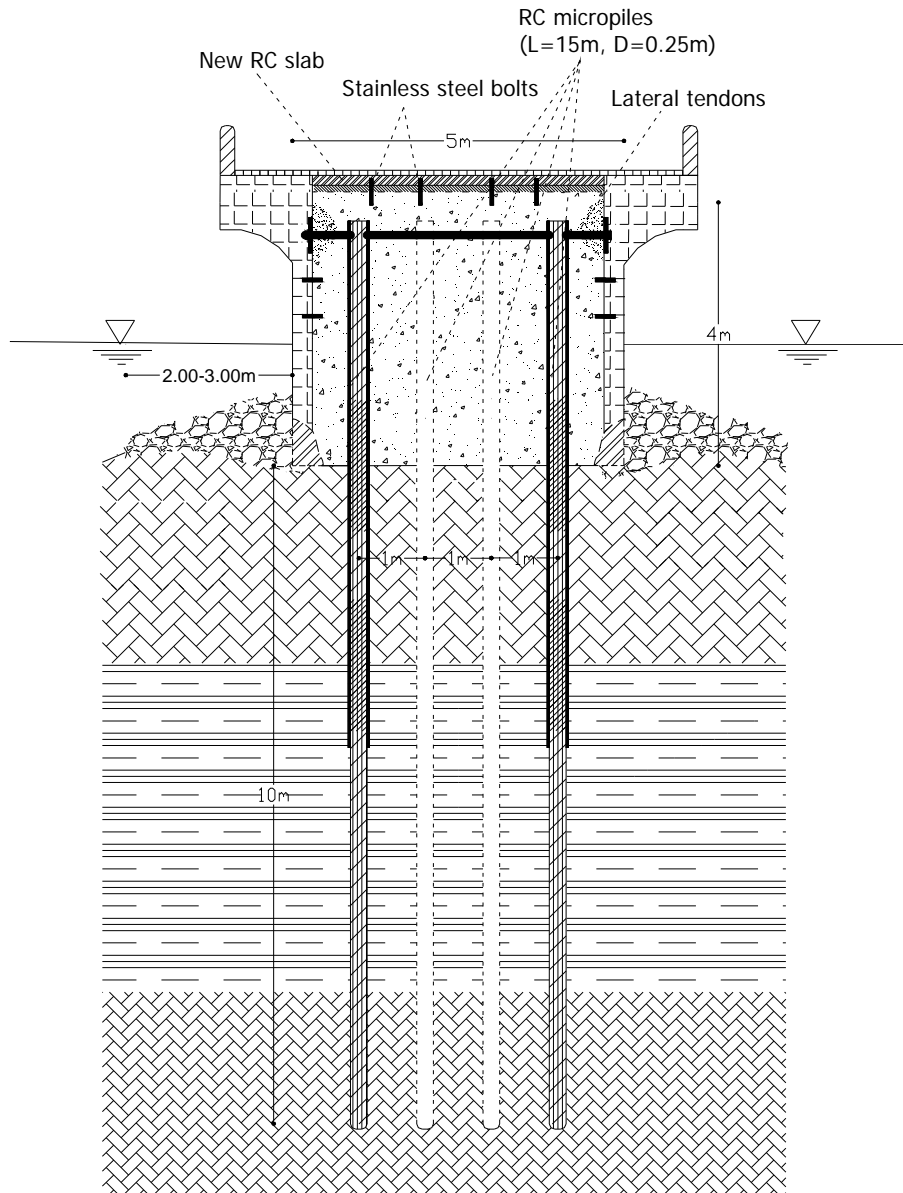
Fig. 12 Typical cross-section of the rehabilitated "De Bosset" bridge showing the proposed intervention measures

steel lateral tendons placed every 1.5 m along the longitudinal axis of the bridge and a new lightly-reinforced concrete slab of 15 cm thickness connected to the original bridge structure through a mesh of stainless steel bolts, allowing for light traffic on the bridge deck. The connection between the new reinforced concrete slab and the piles was deliberately avoided to ensure low bending moments at the piles heads.

The proposed intervention scheme was approved by the Directorate for the Restoration of Byzantine and Post-byzantine Monuments of the Greek Ministry of Culture and was recently

applied at the bridge site. During implementation of the rehabilitation measures, a number of unfavourable site conditions were revealed. More specifically, it was found that the filling material between the longitudinal spandrel walls was extremely heterogeneous composed of soil, sparse steel bars and debris (Fig. 13(a)), making the drilling and the construction of the micropiles particularly difficult. In order to stabilise the sidewalls of the boreholes, steel tubes of 30 cm diameter were employed to prevent debris fall inside the borehole (Fig. 13(b)). Piles reinforcement was introduced through PVC tubes placed within the steel tubes.

The PVC tubes were not removed after casting the micropiles to protect them from strong sea currents. The above technical solution allowed drilling of the micropiles group based on the original design (Fig. 14(a)). For the old stone sections of the bridge, the stainless steel lateral tendons were anchored to new stone walls constructed in the inner side of the stone facades (Fig. 14(b)). With reference to the architectural interventions, the original stone facades of the bridge

Fig. 13 (a) Filling material of the bridge composed of soil, sparse steel bars and debris that was revealed during restoration works (b) Steel tubes embedded consecutively to prevent debris fall inside the borehole during the drilling of the micropiles

Fig. 14 (a) Group of micropiles drilled from the bridge deck (b) Steel plate embedded in the lateral façades of the bridge for anchoring the stainless steel tendons

were conserved whereas the concrete facades were repaired with corrosion -resistant mortars and covered with a thin stone layer of 6 cm thickness.

8.1 Safety factor against bearing capacity of the foundation soil for the rehabilitated bridge

Focusing on the bearing capacity of the bridge foundation soil, the finite-element model of the bridge was reanalyzed taking into account the group of micropiles. Upon assuming negligible pile-to-pile interaction due to the large normalized pile spacing, the micropiles were modelled by a set of point spring supports computed from available analytical solutions for single-pile stiffness (Pender 1993). Modal characteristics of the rehabilitated bridge model are summarized in the column (c) of Table 2. Naturally, the incorporation of the micropiles group increased the overall stiffness of the soil-bridge system, leading to higher effective natural frequencies with respect to the flexible-base case before the interventions. A new series of response spectrum analyses of the soil-micropiles-bridge model was performed to compute the mean vertical stress developed at the foundation of the bridge piers under the same loading scenarios. The results were compared to the bearing capacity of the soil-micropiles system leading to the corresponding safety factors plotted in Fig. 11 for the rehabilitated flexible-base model. The favourable effect of the combined intervention scheme is reflected in the increase of the safety factor against bearing capacity of the foundation soil above unity with respect to the pre-rehabilitation phase.

9. Performance of the rehabilitated bridge under the strong Cephalonia earthquakes of 01/26/2014 and 02/03/2014

On January 26th (13:55GMT) and February 3rd (03:08GMT), 2014 two strong earthquakes of magnitude M6.1 and M6.0, respectively, stroke the Island of Cephalonia, inducing major geotechnical failures and damages on structures and lifelines. Particularly high ground accelerations (up to 0.70 g) were recorded at the peninsula of Paliki (GEER/EERI/ATC Report 2014, Theodulidis *et al.* 2016) which is less than 15 km away from the "De Bosset" bridge, by permanent accelerometric stations and a temporal accelerometric network deployed after the first earthquake of 01/26/2014 by the EPPO-ITSAK team (EPPO-ITSAK reports 2014a, 2014b). Acceleration time histories of the ground motion recorded at the Argostoli (ARG2) station are shown in Figs. 15(a) and 15(b) for the main earthquake events of January 26th and February 3rd, 2014, having peak ground accelerations at 0.35 g and 0.26 g, respectively. The above main events were followed by a large number of aftershocks with maximum magnitude in the order of M5.4.

The rehabilitated bridge was inspected soon after the main earthquake events (Rovithis *et al.* 2014). The inspection revealed no damage or visible defects at the bridge structure (Fig. 16) indicating an overall satisfactory seismic performance, despite the large ground accelerations experienced in this site. On the contrary, the quay wall adjacent to the "De Bosset" bridge founded on the same soil conditions suffered permanent horizontal displacement of 10cm towards the shoreline with an approximate backfill settlement of 15 cm after the first earthquake event of 01/26/2014. The observed lateral movement of the quay wall and the settlement of the backfill were further increased, almost doubled at some locations, after the second earthquake of 02/03/2014 (Fig. 17).

Given the comparable geological setting between ARG2 and CH accelerometric station sites, the recorded motions at ARG2 station were deconvoluted to the bedrock level by implementing
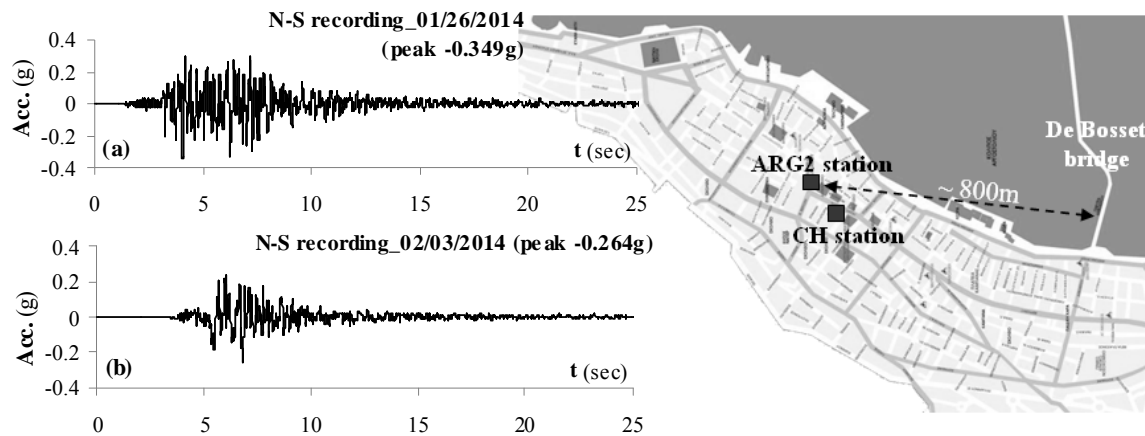
Fig. 15 Acceleration time histories (N-S component) recorded at Argostoli (ARG2) station for (a) the mainshock of 01/26/2014 (13:55GMT) and (b) the mainshock of 02/03/2014 (03:08GMT) (EPPO-ITSAK reports 2014a, 2014b)

Fig. 16 In-situ inspection of the rehabilitated "De Bosset" bridge after the two major Cephalonia earthquakes of 01/26/2014 and 02/03/2014, revealing no damage or visible defects at the bridge structure

the soil profile at the CH station. Acceleration time histories computed at the bedrock level are plotted in Figs. 18(a) and 18(b), having peak values at 0.174 g and 0.146 g for the earthquake events of 01/26/2014 and 02/03/2014, respectively. The deconvoluted rock mothins were then specified at the base of the bridge soil profile to compute the seismic response at the ground surface of the bridge site by means of equivalent linear soil response analysis (Modaressi and Foerster 2000). Figs. 18(c) and 18(d) show the computed acceleration time histories at the ground surface of the bridge site with peak values equal to 0.371 g and 0.251 g for the first and the second earthquake, respectively. The corresponding surface-to-bedrock peak ground acceleration ratio is close to two, in agreement with the mean amplification ratio obtained during the design of the rehabilitation measures (Fig. 7(b)).

In complements to the visual evidence on the effectiveness of the rehabilitation measures, the bridge response under the seismic loading imposed by each earthquake was further explored by

Fig. 17 Recorded failures adjacent to the "De Bosset" bridge; permanent lateral displacement of the quay wall and settlement of the backfill induced by (a) the first M6.1 earthquake event of 26/01/2014 (13:55GMT) and (b) the second M6.0 earthquake event of 03/02/2014(03:08GMT)
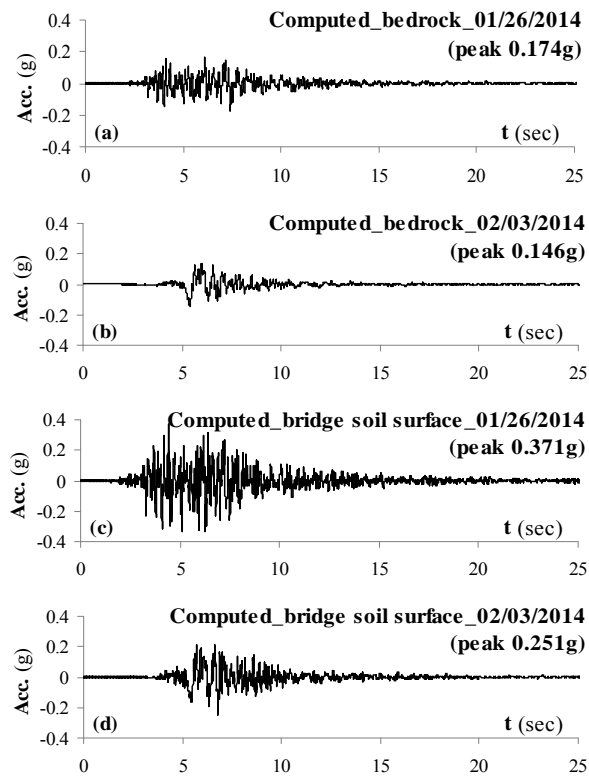
Fig. 18 (a, b) Acceleration time histories computed at the bedrock of the CH station soil profile for the two earthquake events of (a) 01/26/2014 and (b) 02/03/2014. (c, d) Acceleration time histories computed at the surface of the bridge soil profile for the two earthquake events of (c) 01/26/2014 and (d) 02/03/2014
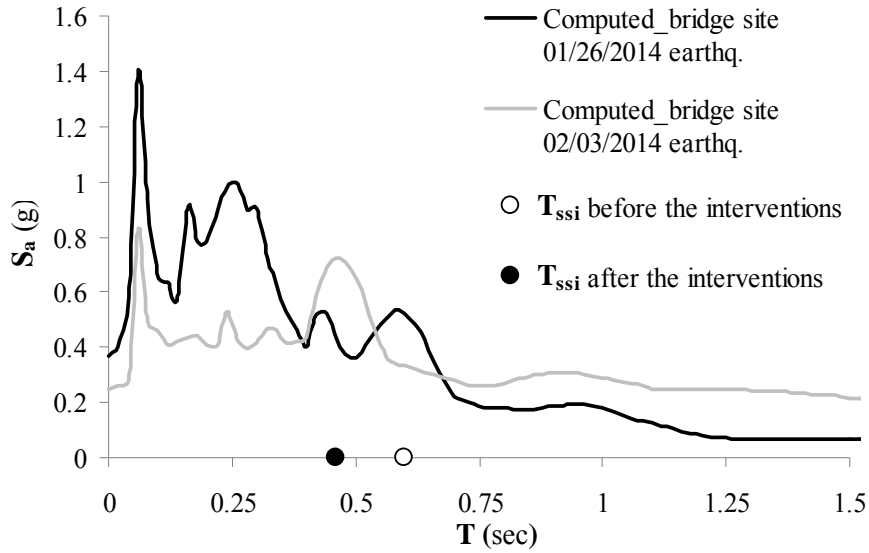
Fig 19. Acceleration response spectra of the two earthquake motions computed at the foundation level of the bridge; the effective natural period (T_{ssi}) of the flexible-base bridge model before and after the intervention measures is also shown
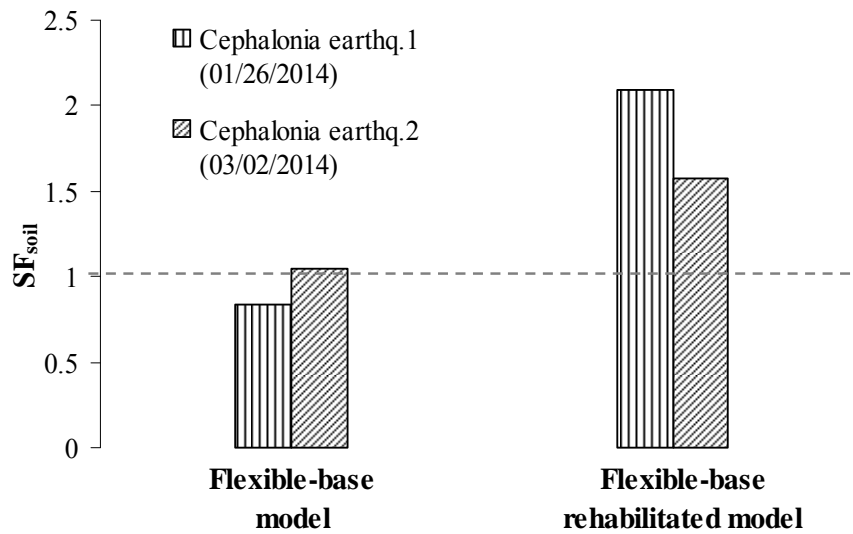
Fig. 20 Effect of rehabilitation measures on the bridge safety factor against bearing capacity of the foundation soil under the computed seismic loading induced by the two earthquakes of 01/26/2014 and 02/03/2014

implementing the 3D numerical model of the bridge. The corresponding acceleration response spectra specified at the base of the bridge model are compared in Fig. 19. The effective natural periods (T_{ssi}) of the pre- and post-rehabilitated bridge model under flexible-base conditions are also noted in the graph, referring to the fundamental vibrational mode (Table 2). It is observed that

the rehabilitated bridge sustained larger seismic loading under the second earthquake of 03/02/2014, due to the decrease of the effective natural period after the intervention measures. The above is reflected in the safety factor against bearing capacity of the foundation soil (SF_{soil}) computed for the second earthquake (Fig. 20), which is lower than the SF_{soil} obtained for the first earthquake. However, for both earthquake events, SF_{soil} is increased above unity with respect to the pre-rehabilitation model response, indicating the capacity of the bridge foundation system after the interventions to withstand safely the imposed seismic loading.

10. Conclusions

A rather complicated and efficient retrofitting scheme was presented for the old stone masonry "De Bosset" bridge founded on unfavourable soil conditions in the particularly high-seismicity region of Cephalonia Island in Greece. The comprehensive survey and reconnaissance campaigns and studies undertaken to evaluate the pathology and the seismic performance of the bridge were described. Simplified methods of transverse failure assessment and stress-based finite-element analyses were implemented to investigate the structural stability of the bridge, leading to a set of rehabilitation measures by combining structural strengthening and foundation soil improvement. Special attention was paid to the preservation of the architectural, archaeological and aesthetic features of the monument. The detailed study of the bridge pathology and the design of the intervention measures revealed the following important points:

• In-situ inspection and testing of structural materials and foundation soil for old stone masonry bridges was particularly critical for the "De Bosset" bridge, revealing a highly deteriorated structure founded on a low-strength and deformable soil. The above delineated the design of the rehabilitation scheme, requiring structural strengthening and upgrade of the foundation bearing capacity.

• Soil-structure interaction may possess a key role in controlling the vibrational characteristics of such type of structures that should be considered during the design of the intervention measures. In the case study of the "De Bosset" bridge, the incorporation of the soft foundation soil modified substantially the vibrational characteristics of the massive structure, leading to a considerable increase of its effective natural period with respect to the fixed-base case.

• The inadequate transverse strength associated with the out-of-plane failure mechanism of the bridge spandrel walls was identified as a major detrimental factor during the assessment of the bridge seismic stability.

• The proposed rehabilitation scheme combines foundation soil improvement with micropiles and structural strengthening mainly with transverse stainless steel tendons connecting the spandrel walls of the bridge. The latter contributed to the monolithic behaviour of the structure in the transverse direction by partially disallowing out-of-plane deformation. The retrofitting measures are complemented by the reconstruction of the masonry walls and the protection of the piers foundation against future scouring with stone-gravel material.

• The rehabilitated "De Bosset" bridge sustained successfully the two strong M6.1 and M6.0 earthquakes that stroke the Island of Cephalonia on 26/01/2014 and 03/02/2014, respectively, with no damages or visible defects, indicating a very satisfactory seismic performance, despite the high ground accelerations experienced in this site. Further evidence on the efficiency of the intervention measures was provided by numerical analysis of the bridge seismic response using ground motion records of the two seismic events.

Acknowledgements

References

ANSYS Inc. (2001), *ANSYS User's manual*, SAS IP, Houston, USA.

Asteris, P.G., Chronopoulos, M.P., Chrysostomou, C.Z., Varum, H., Plevris, V., Kyriakides, N. and Silva, V. (2014), "Seismic vulnerability assessment of historical masonry structural systems", *Eng. Struct.*, **62**, 118-134.

AUTH-ITSAK (1996), *Final report on Study of the effect of local soil conditions, geomorphology and soil structure interaction on the recordings of the National Accelerographic Network*.

Barros, F. and Luco, J. (1995), "Identification of foundation impedance functions and soil properties from forced vibration tests on Hualien containment model", *Soil Dyn. Earthq. Eng.*, **14**(4), 229-248.

Brencich, A. and Colla, C. (2002), "The influence of construction technology on the mechanics of masonry railway bridges", *Proceedings of the 5th International Conference on Railway Engineering*, London.

Cakir, F. and Seker, B. (2015), "Structural performance of renovated masonry low bridge in Amasya, Turkey", *Earthq. Struct.*, **8**(6), 1387-1406.

CEN (2002), European Committee for Standardization *Eurocode 8 Design of Structures for Earthquake Resistance, Part 5: Foundations, Retaining structures and Geotechnical Aspects*, Brussels.

Code of Practice for Structural Use of Masonry (1992), Part 1: Unreinforced Masonry, BS 5628-1, British Standards Institution, London,.

EAK2000, *Greek Seismic Code*, OASP, Athens.

EPPO-ITSAK (2014a), "The earthquake of 26/01/2014 (M6.1) in Cephalonia (Greece): Strong ground motion, soil behaviour and response of structures", Available online at http://www.itsak.gr/en/news/news/70.

EPPO-ITSAK (2014b), "Strong ground motion of the February 3, 2014 (M6.0) Cephalonia earthquake: Effects on soil and built environment in combination with the January 26, 2014 (M6.1) event", Available online at http://www.itsak.gr/en/news/news/79.

Erdogmus, E. and Boothby, T. (2004), "Strength of spandrel walls in masonry arch bridges", *Transport. Res. Record: J. Transport. Res. Board*, **1892**, 47-55.

Gazetas, G. (1991), "Formulas and charts for impedance functions of surface and embedded foundation", *J. Geotech. Eng.*, ASCE, **117**(9), 1363-1381.

GEER/EERI/ATC (2014), "Earthquake Reconnaissance January 26th/February 3rd 2014 Cephalonia", Greece Events, Report Version 1.

Griffith, M., Magenes, G., Melis, G. and Picchi, L. (2003), "Evaluation of out-of-plane stability of

unreinforced masonry walls subjected to seismic excitation", *J. Earthq. Eng.*, **7**(1), 141-169.

Krstevska, L.S., Kustura, M. and Tashkov, L.A. (2008), "Experimental in-situ testing of reconstructed old bridge in Mostar", *Proceedings of the 14th World Conference on Earthquake Engineering*, Beijing.

Modaressi, H. and Foerster, E. (2000), *Cyberquake: User's Manual*, BRGM, France.

Mononobe, N. and Matsuo, O. (1929), "On the determination of earth pressure during earthquakes", *Proceedings of the World Engineering Congress*, Tokyo.

Okabe, S. (1924), "General theory on earth pressure and seismic stability of retaining walls and dams", *J. JSCE*, **10**(6), 1277-1323.

OPCM 3274. (2005), Ordinanza del Presidente del Consiglio dei Ministri n. 3274 del 20 Marzo 2003: Primi elementi in materia di criteri generali per la classificazione sismica del territorio nazionale e di normative tecniche per le costruzioni in zona sismica (ANNEX 11.D).

Page, J. (1993), "Repair and strengthening of masonry arches", *Proceedings of the IABSE Symposium on Structural Preservation of the Architectural Heritage*, Rome.

Papayianni, I., Pachta, V. and Alexiou, A. (2007), "Study of the constructing materials, techniques and pathology symptoms of the stone bridge De Bosset in Kefalonia", *Proceedings of the 5th International Conference on Arch Bridges*, Madeira.

Papazachos, B. (1997), *Earthquakes of Greece.* Ziti publications, Thessaloniki.

Preciado, A., Bartoli, G. and Budelmann, H. (2015), "Fundamental aspects on the seismic vulnerability of ancient masonry towers and retrofitting techniques", *Earthq. Struct.*, **9**(2), 339-352.

Pender, M.J. (1993), "Aseismic pile foundation design analysis", *Bull. NZ. Nat'l Soc. Earthq. Eng.*, **26**(1), 49-161.

Pitilakis, K. (2006), "Rehabilitation and Reinforcement Study of DeBosset bridge at Argostoli, Cephalonia", Final Report submitted to Directorate for the Restoration of Byzantine and Postbyzantine Monuments, Greek Ministry of Culture, 240.

Proske, D. and Van Gelder, P. (2009), *Safety of Historical Stone Arch Bridges*, Springer Publications.

Roesset, J.M. (1976), "Soil amplification of earthquakes", (Ed.) C.S., Desai and J.T., Christian, *Numerical methods in geotechnical engineering*, New York: McGraw-Hill.

Rota, M., Pecker, A., Bolognini, D. and Pinho, R. (2005) "A methodology for seismic vulnerability of masonry arch bridge walls", *J. Earthq. Eng.*, **9**(2), 331-353.

Rovithis, E. and Pitilakis, K. (2011), "Seismic performance and rehabilitation of old stone bridges in earthquake-prone areas: the case of Debosset bridge in Greece", *Proceedings of the 1st International Conference on Bridges, Innovations on Bridges and Soil-Bridge Interaction*, Athens.

Rovithis, E., Pitilakis, K. and Apostolidis, P. (2006), "Rehabilitation of the historic bridge De-Bosset in Argostoli", *Proceedings of the 1st Hellenic Conference on restoration of monuments*, ETEPAM, Thessaloniki.

Rovithis, E., Pitilakis, K., Vlachoulis, T., Karani, I., Chorafa, E. and Zarogiani, E. (2014), "De Bosset monumental stone bridge in Cephalonia: Strengthening measures and seismic response under the earthquakes of 26/01/2014 and 03/02/2014", *Proceedings of the 2nd International Conference on Bridges, Innovations on Bridges and Soil-Bridge Interaction*, Athens.

Theodoulidis, N., Karakostas, Ch., Lekidis, V., Makra, K., Margaris, B., Morfidis, K., Papaioannou, Ch., Rovithis, Emm., Salonikios, T. and Savvaidis, A. (2016), "The Cephalonia, Greece, January 26 (M6.1) and February 3(M6.0) earthquakes: Near field ground motion and effects on soil and structures", *Bull. Earthq. Eng.*, **14**(1), 1-38.

SA